Cell, Vol. 90, 235–245, July 25, 1997, Copyright ©1997 by Cell Press

Costal2, a Novel Kinesin-Related Protein in the Hedgehog Signaling Pathway

John C. Sisson,* Karen S. Ho, Kaye Suyama, and Matthew P. Scott
Departments of Developmental Biology and Genetics
Howard Hughes Medical Institute
Stanford University School of Medicine
Stanford, California 94305-5427

Summary

The Hedgehog (HH) signaling proteins control cell fates and patterning during animal development. In Drosophila, HH protein induces the transcription of target genes encoding secondary signals such as DPP and WG proteins by opposing a repressor system. The repressors include Costal2, protein kinase A, and the HH receptor Patched. Like HH, the kinase Fused and the transcription factor Cubitus interruptus (CI) act positively upon targets. Here we show that *costal2* encodes a kinesin-related protein that accumulates preferentially in cells capable of responding to HH. COS2 is cytoplasmic and binds microtubules. We find that CI associates with COS2 in a large protein complex, suggesting that COS2 directly controls the activity of CI.

Introduction

Animal development employs localized sources of HH signals to organize pattern by controlling cell fates in the embryo. Early in Drosophila development, embryonic segments and nascent imaginal discs are divided into anterior compartment (A) cells that transcribe *cubitus interruptus* (*ci*), a zinc-finger-containing transcription factor (Eaton and Kornberg, 1990; Orenic et al., 1990) and posterior (P) compartment cells that transcribe *engrailed* (*en*), a homeobox containing transcription factor (Poole et al., 1985). HH signal, emanating from P cells, maintains the transcription of the signaling molecules *wingless* (*wg*) in embryonic segments and leg imaginal discs and *decapentaplegic* (*dpp*) in leg and wing imaginal discs along the A/P border (Basler and Struhl, 1994; Capdevila et al., 1994; Tabata and Kornberg, 1994). The precisely defined sources of WG and DPP near the A/P boundary pattern surrounding tissue.

HH signal transduction employs a set of activators and repressors of HH target gene transcription (Hammerschmidt et al., 1997). In addition to HH, components required for activation include a seven transmembrane protein, Smoothened (SMO) (Alcedo et al., 1996; van den Heuvel and Ingham, 1996), the kinase Fused (FU) (Préat et al., 1990; Thérond et al., 1993, 1996), and CI. Components required for target gene repression include the transmembrane protein Patched (PTC) (Hooper and Scott, 1989; Nakano et al., 1989), protein kinase A (PKA) (Jiang and Struhl, 1995; Lepage et al., 1995; Li et al., 1995; Pan and Rubin, 1995), and the product of *costal2* (*cos2*) (Whittle, 1976; Grau and Simpson, 1987; Simpson and Grau, 1987; Forbes et al., 1993; Capdevila et al., 1994).

cos2 is a maternal effect gene and a zygotic lethal. Removal of the maternal and zygotic contributions of *cos2* causes embryos to die with a cuticle pattern similar to that of *ptc* homozygous embryos (Grau and Simpson, 1987). As in *ptc* mutants, *cos2* mutant embryos have expanded transcription domains of the HH target gene *wg* (Forbes et al., 1993) and mirror-image pattern duplications in the central part of each segment (Grau and Simpson, 1987). In adults, *cos2* mutations cause ectopic *dpp* expression (Capdevila et al., 1994) and duplications of wings, halteres, legs, and antennae (Whittle, 1976; Grau and Simpson, 1987; Simpson and Grau, 1987). The adult phenotypes are similar to those seen when *ptc* function is eliminated or when HH is overexpressed (Basler and Struhl, 1994; Ingham and Fietz, 1995). Strong allele-specific genetic interactions with *fu* suggest that *cos2* may function in the cytoplasm of A cells in parallel with or downstream of *fu* (Préat et al., 1993).

When HH signal is received by A cells, an increase in FU activity and a decrease in COS2 activity are thought to allow CI to directly activate the transcription of HH target genes. CI levels are posttranscriptionally elevated along the A/P border in response to HH signal (Motzny and Holmgren, 1995; Slusarski et al., 1995), an apparent indicator of its activation as a transcription factor (Alexandre et al., 1996; Dominguez et al., 1996; Hepker et al., 1997). However, most CI detectable by antibody staining is observed in the cytoplasm (Motzny and Holmgren, 1995; Slusarski et al., 1995). Even with high level HH signaling, little, if any, CI is visible in the nucleus, suggesting that either a small amount of CI is sufficient to activate targets or nuclear CI is masked from antibody detection.

In this paper, we focus on COS2 and its relationship with CI. We have found that COS2 is related to the kinesin superfamily of proteins and binds strongly to microtubules. COS2 is present at high levels in the cytoplasm of A cells where CI is expressed. COS2 is associated with CI in a large protein complex, suggesting that COS2 constitutes part of a system for regulating the activity of CI. These studies suggest a novel role for kinesin-related proteins in regulating signal transduction.

Results

Molecular Identification of *cos2*

cos2 is located on the right arm of the second chromosome within polytene interval 43B2; 43C1.2 (Grau and Simpson, 1987; Heitzler et al., 1993). A chromosome walk was initiated from a chromosome position proximal to *cos2* at 43B1 (Figure 1A). *Df(2R)sple*^{D1} (43A1.2; 43B2) and *Df(2R)NCX11* (43C1.2; 44C1.2) complement

*Present Address: Department of Biology, Sinsheimer Laboratories, University of California, Santa Cruz, California 95064.

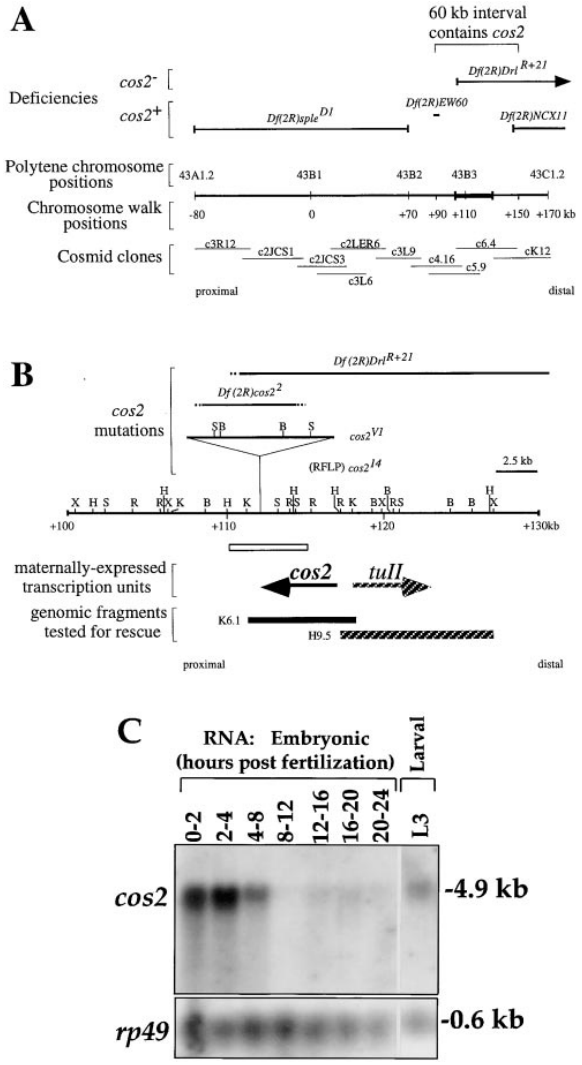

Figure 1. Molecular Map of the *cos2* Region and *cos2* Transcript Expression

(A) Thick horizontal bars (top) indicate the positions of four deficiencies relative to polytene chromosome positions and corresponding chromosome walk positions (middle). Thin horizontal bars (bottom) indicate the positions of overlapping cosmid clones. *cos2* lies within a 60 kb interval between *Df(2R)EW60* and *Df(2R)NCX11*. The thick line within this interval, overlapping 43B3 ($^{+}$110), is enlarged in (B).

(B) Four *cos2* mutations are close to two maternally expressed transcription units. Thick horizontal bars above the restriction map indicate positions of *cos2* mutations. Hatching indicates uncertain deficiency endpoints. *Df(2R)Drl*$^{R+21}$ and *Df(2R)cos2*^{2} define a 5 kb interval (open bar) containing a portion of *cos2*. *cos2*^{V1} is an insertion, and *cos2*^{14} is associated with RFLPs within a 1.9 kb EcoRI fragment. Thick arrows below the restriction endonuclease map indicate the positions and directions of transcription of *cos2* and tuII. A 6.1 kb KpnI genomic fragment (K6.1, closed bar) fully rescues *cos2* embryonic lethality to adulthood. A 9.5 kb HindIII genomic fragment (H9.5, hatched bar) fails to rescue *cos2* embryonic lethality. (B) = BamHI, (H) = HindIII, (K) = KpnI, (R) = EcoRI, (S) = SalI, and (X) = XbaI.

(C) A blot containing total RNA from different embryonic stages and third instar larvae was hybridized to radioactive *cos2* and *rp49* probes. The *cos2* probe reveals a single 4.9 kb transcript. *rp49* serves as a loading control (O'Connell and Rosbash, 1984).

cos2 mutations and bracket the *cos2* locus. The chromosome walk spans the distance between their adjacent deficiency endpoints at positions $^{+}$70 and $^{+}$150 kb. *Df(2R)EW60* complements *cos2* mutations and removes DNA centered over position $^{+}$90 (Figure 1A). *Df(2R)Drl*$^{R+21}$ fails to complement *cos2* mutations and lies distal of *Df(2R)EW60*. Together *Df(2R)EW60* and *Df(2R)NCX11* limit the DNA interval containing *cos2* to 60 kb (Figure 1A, horizontal bracket).

An analysis of the 60 kb region with genomic DNA blots reveals restriction fragment length polymorphisms (RFLPs) for several *cos2* mutations and places part or all of *cos2* within a 5 kb interval of DNA (Figure 1B, open bar). *Df(2R)cos2*^{2} behaves as an amorphic allele of *cos2*(Grau and Simpson, 1987) and has a 6.5 kb DNA deletion between positions $^{+}$108 and $^{+}$115. *Df(2R)Drl*$^{R+21}$ (Heitzler et al., 1993) has a proximal endpoint that lies within the *Df(2R)cos2*^{2} deletion, between $^{+}$110 and $^{+}$111. Therefore, part or all of *cos2* must lie within the 5 kb region of their overlap, between $^{+}$110 and $^{+}$115. Two additional *cos2* alleles map to this region. *cos2*^{V1} is a viable allele that displays adult pattern duplications in the presence of semidominant alleles of *Cos1* (Grau and Simpson, 1987; Simpson and Grau, 1987). *cos2*^{V1} is associated with a 9 kb insertion at position $^{+}$112. In addition, *cos2*^{14}, a strong hypomorphic allele (Heitzler et al., 1993), is associated with RFLPs between $^{+}$115 and $^{+}$117.

cos2 is maternally active (Grau and Simpson, 1987), so *cos2* mRNA is likely to be present in early embryos prior to the onset of zygotic transcription at 2.5 hr after fertilization. Radioactive cDNA synthesized from 0–2 hr, 4–8 hr, or 8–16 hr embryonic poly(A)$^{+}$ RNA was hybridized to blots containing the 60 kb *cos2* region. Two contiguous SalI fragments (1.2 kb and 6.3 kb) that overlap the 5 kb *cos2* region hybridize to the 0–2 hr cDNA probe (Figure 1B). cDNA clones overlapping the large SalI fragment were recovered for two adjacent, divergently transcribed, maternally expressed transcription units (Figure 1B).

To determine which transcription unit is *cos2*, genomic fragments containing either the proximal or distal transcription unit were tested for their ability to rescue *cos2* embryonic lethality. Transgenic flies were constructed carrying either a 6.1 kb genomic KpnI fragment (K6.1) containing the proximal transcription unit or a 9.5 kb genomic HindIII fragment (H9.5) containing the distal transcription unit (Figure 1B). In a cross of *cos2*^{2}/*CyO* to *cos2*^{12}/*CyO* stocks, no homozygotes survive compared to 431 heterozygous progeny. When the same cross was done in the presence of one copy of K6.1, the adult progeny were composed of 1050 heterozygotes, zero homozygotes without K6.1, and 297 homozygotes carrying K6.1. The expected number of *cos2* homozygotes was 525, and half of these should carry K6.1, so the results suggest that K6.1 contains all or a substantial proportion of *cos2*. H9.5 does not rescue *cos2* embryonic lethality (data not shown).

A 4.8 kb *cos2* cDNA hybridizes to a 4.9 kb transcript present at high levels during the first four hours of embryogenesis (Figure 1C), moderate levels between four and twelve hours, and low levels for the duration of embryogenesis. The transcript is also present during the third larval instar.

cos2 Encodes a Kinesin Heavy Chain–Related Protein

The complete sequence of a 4.8 kb cDNA clone for *cos2* was determined, as was all of the genomic sequence flanking the cDNA in the rescuing transgene. The cDNA sequence reveals a single, large open reading frame (ORF). The putative translational start site matches the Drosophila consensus sequence well and contains codons common in other Drosophila genes (Cavener, 1987; Ashburner, 1989). Multiple stop codons in all three reading frames are present upstream of the putative start codon (data not shown). The surrounding genomic sequence contains three short ORFs that do not begin with methionine or match the usual pattern of Drosophila codon usage.

cos2 is predicted to encode a 1201 amino acid polypeptide with a molecular weight of 133 kDa (Figure 2A). The N-terminal (residues 1–450) and C-terminal (residues 1050–1201) regions are predicted to form globular structures consisting of alternating α helices and β sheets (Figure 2B, MacVector 4.1.1, Kodak). The central region (residues 643–990) contains 36 heptad repeats (Figure 2A, underlined) that are predicted to mediate the formation of a stable homodimer through a parallel coiled coil (Figure 2B) (Woolfson and Alber, 1995).

COS2 is similar to members of the kinesin protein family (Figure 2C). Over a span of 254 N-terminal amino acids (residues 136–389), COS2 is 25%–30% identical to the motor domains of different members of the kinesin gene family (Figure 2C, right column) (Higgins et al., 1992). Kinesins are molecular motor proteins that move along microtubules powered by ATP hydrolysis (reviewed by Goldstein, 1993; Moore and Endow, 1996). Conventional kinesin consists of two kinesin heavy chains (KHC) and two kinesin light chains (KLC). KHC consists of an N-terminal motor domain, a central domain made up of heptad repeats, and a C-terminal putative "cargo" domain thought to bind vesicles to move them. The motor domain of KHC is sufficient to mediate ATP-dependent movement along microtubules in vitro (Yang et al., 1990).

Several motor domain motifs implicated in nucleotide (N) or microtubule binding are highly conserved within the kinesin family (Goldstein, 1993; Sablin et al., 1996; Vale, 1996) and are generally conserved in COS2. For example, the nucleotide-binding motif 1 (N1 or P loop) in COS2 is 50% identical to the kinesin gene family consensus sequence (Figures 2A [shaded box] and 2C). Four residues strictly conserved in the family (Goldstein, 1993) are present in COS2 (Figure 2C, thin underlining), but COS2 residues R177 and Q179 are significantly different. The N2 motif, SSRSH, in COS2 is replaced by SLPAH (Figure 2A, thick underline), while N3, DLAGS/TE, is conserved in COS2 (Figure 2A, stippled underline). N4 is not present in COS2. At least two motifs have been tentatively implicated in microtubule binding (Sablin et al., 1996; Woehlke et al., 1997 [this issue of *Cell*]): the strictly conserved DLL motif and the L12 motif (Figure 2A, open boxes) (Sablin et al., 1996). The L12 consensus sequence is $\Phi_{I/V}P_{Y/F}R_{N/D}$ (Φ = hydrophobic residues), and both the P and R residues are strictly conserved (Goldstein, 1993). In COS2, the DLL motif is present while L12 is partially conserved, with the expected R being absent.

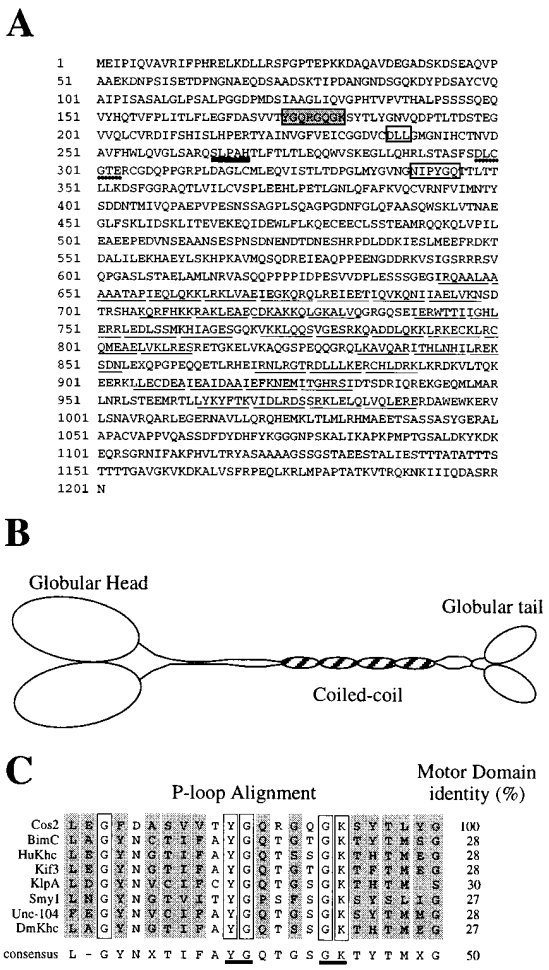

Figure 2. COS2 Amino Acid Sequence, Analysis, and Alignments

(A) *cos2* is predicted to encode a 1201 amino acid protein. The N terminus contains three putative nucleotide-binding motifs (N1 [P loop], shaded box; N2, thick underline; and N3, stippled underline) (Vale, 1996) and two putative microtubule-binding motifs (open boxes) (Sablin et al., 1996). The central portion contains 36 heptad repeats arranged in eight clusters (thin underlining).

(B) The predicted structure of COS2. Sequence analyses predict that the N and C termini adopt globular conformations and that the 36 heptad repeats mediate the formation of a homodimer by forming a parallel coiled coil.

(C) Alignment of the putative *cos2* P-loop motif (N1) with those of representative members of the kinesin gene family. A consensus sequence for the family is shown at the bottom. Closed and shaded rectangles indicate identity and similarity, respectively. The four underlined residues are invariant within the kinesin gene family (Goldstein, 1993). The minus sign indicates an acidic residue, and (X) indicates the absence of a consensus residue. The percent identity between *cos2* and the indicated kinesin family members is shown at the right.

COS2 Expression Prior to Germ Band Extension

Polyclonal rat antisera were raised against N- and C-terminal portions of COS2. Both antisera were affinity purified and used to probe blots of embryo protein extracts. Both antisera reveal a single band of 175 kDa (Figure 3A). Preimmune antisera do not detect any protein on these blots (data not shown). COS2 migrates much more slowly than its predicted size of 133 kDa,

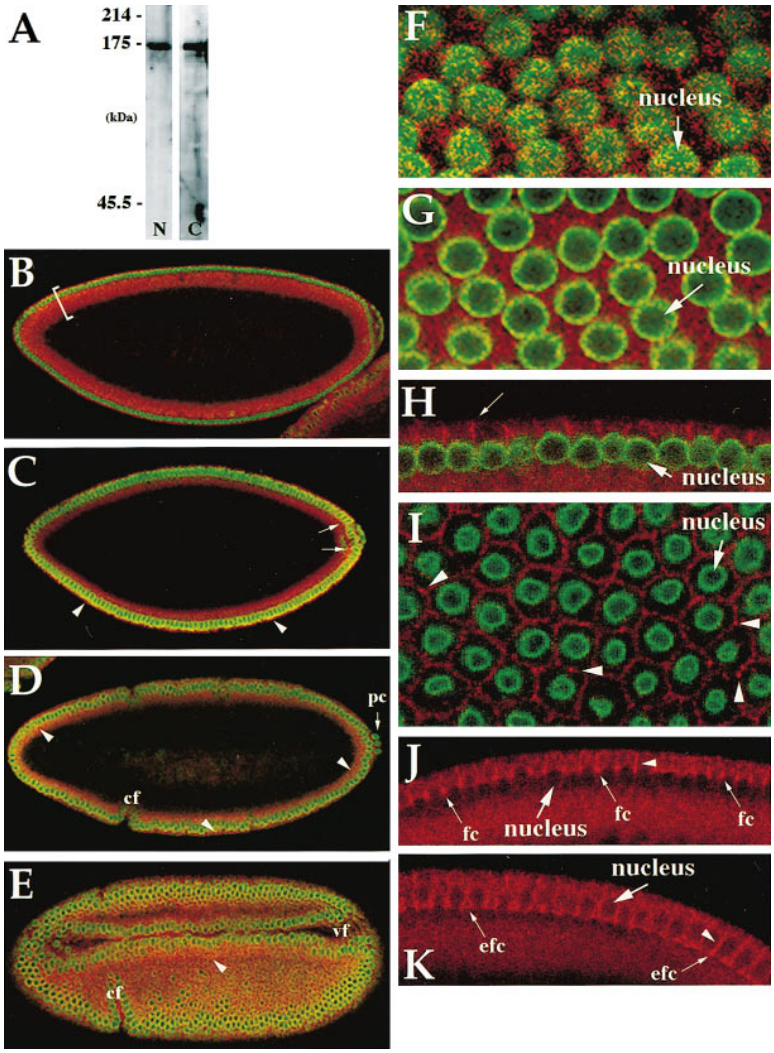

Figure 3. The Spatial Distribution of COS2 in the Early Embryo

(A) Affinity-purified anti-N-terminal (N) and anti-C-terminal (C) COS2 antisera recognize a single major protein band of 175 kDa on protein blots.

(B–E) Methanol-fixed embryos were incubated with affinity-purified anti-COS2 (red) and anti-lamin (green) antibodies and detected by indirect immunofluorescence using a scanning confocal microscope. Anterior is to the left and dorsal is up. (pc) = pole cells, (cf) = cephalic furrow, and (vf) = ventral furrow. COS2 is present along the periphery of stage 4 (B) and stage 5 (C) embryos surrounding somatic nuclei (bracket). COS2 can be seen in the apical cytoplasm of newly forming cells ([C], arrowheads) and at enhanced levels along the basal face of elongated nuclei in stage 5 embryos (arrows). COS2 is present in all cells of stage 6 embryos (D and E; arrowheads). In (E), an optical section through the apices of presumptive epidermal cells reveals uniform levels of COS2 (arrow).

(F and G) Optical sections at apical (F) and basal (G) focal planes, parallel with the surface of an early stage 4 embryo, show COS2 uniformly distributed within the cytoplasm.

(H and I) COS2 accumulates between and apical of nuclei in late stage 4 embryos. In (H), a lateral view shows COS2 as vertical rays (arrow). In (I), a surface view shows COS2 in a honeycomb pattern. Punctate staining is seen along the honeycomb pattern (arrowhead).

(J) During early cellularization, COS2 staining is elevated in furrow canals (arrows). The arrowhead indicates the position of newly formed membrane.

(K) During late cellularization, COS2 staining is elevated in expanded furrow canals along the basal face of nuclei (fc; arrows); in slightly older embryos, COS2 staining forms a line that circumscribes the inner yolk ([C], arrows). Embryos were staged according to Campos-Ortega and Hartenstein (1985).

perhaps due to posttranslational modification. Both antisera also recognize endogenous and overexpressed COS2 in the cytoplasm of Drosophila S2-cultured cells (data not shown).

Both affinity-purified antisera were used to assess the expression of COS2 in early embryos, and both give the same results. In syncytial stage embryos (stage 4), prior to cellularization, COS2 is distributed uniformly within the cortical cytoplasm (Figure 3B, bracket), at apical (Figure 3F) and basal (Figure 3G) focal planes. Anti-lamin antibody (green) outlines the nuclei. COS2 is detected neither within nuclei (Figures 3G–3I) nor in association with microtubule spindles (data not shown). In late syncytial blastoderm embryos just prior to cellularization, COS2 accumulates between, and apical to, nuclei (Figures 3H and 3I). A lateral view shows COS2 accumulation forming rays perpendicular to the surface of the embryo (Figure 3H, arrow). Surface views along the apices of nuclei show COS2 accumulation forming a honeycomb pattern (Figure 3I). COS2 is punctate rather than uniform within the honeycomb lattice (arrowheads).

COS2 is associated with furrow canals throughout cellularization (Figures 3J and 3K). Furrow canals (fc) are located at the leading edge of newly forming membrane between adjacent somatic nuclei (Foe et al., 1993). During cellularization, furrow canals move toward the basal end of the nuclei where they broaden, forming expanded furrow canals (efc), and then fuse with one another in a process that will seal off the new cells from the embryo's interior. COS2 is present at relatively high levels within each early furrow canal (Figure 3J, arrows). At this time, COS2 is also distributed uniformly at lower levels throughout the cortical cytoplasm and along new membrane trailing each furrow canal (Figure 3J, arrowhead). COS2 is associated with expanded furrow canals prior to (Figure 3K, arrows) and after their fusion during late cellularization (Figure 3C, arrows). In cellular blastoderm embryos (Figure 3C, arrowheads) and after the onset of gastrulation, COS2 is in the cytoplasm (Figures 3D and 3E, arrowheads) and at the periphery of all cells (Figure 5C). *cos2* transcripts are uniformly distributed in the early embryo (data not shown).

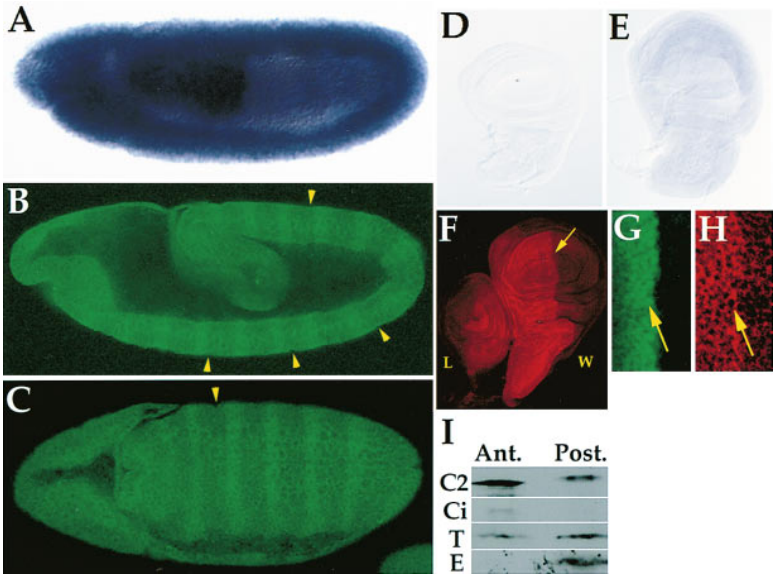

Figure 4. COS2 Is Expressed at Elevated Levels in Anterior Compartment Cells

(A) In situ hybridization of a *cos2* antisense riboprobe to a stage 10 embryo showing uniform levels of *cos2* transcript.

(B and C) COS2 staining in stage 10 embryos. Lateral (B) and dorsal (C) views show COS2 expressed in stripes. The arrowheads indicate morphologically visible parasegmental grooves.

(D and E) In situ hybridization of *cos2* sense (D) and antisense (E) riboprobes to wild-type wing imaginal discs.

(F) COS2 staining in wild-type leg (L) and wing (w) imaginal discs. An arrow indicates the position of the anterior-posterior compartment border.

(G and H) The anterior-posterior compartment border of a *ptc-lacZ* wing imaginal disc stained with both β-gal and COS2 antibodies, respectively. The anterior compartment is at the left in both panels. In (G), β-gal staining is in a narrow band of cells within the anterior compartment along the anterior-posterior compartment border (arrow). In (H), elevated COS2 staining is restricted to the anterior compartment (arrow). Arrows in (G) and (H) are in corresponding positions.

(I) Protein blot of anterior (Ant.) and posterior (Post.) wing disc fragment extracts probed with antibodies to COS2 (C2), CI, α-tubulin (T), and Engrailed (E). COS2, CI, and Engrailed are normalized to tubulin.

COS2 Levels Are Elevated in the Anterior Compartments of Embryonic Segments and Imaginal Discs

In contrast to the uniform distribution of *cos2* mRNA in the germband-extended embryo (Figure 4A), COS2 protein is present in a striped pattern. Faint stripes along the germband are first observed in late stage 9 embryos and become prominent by stage 10 (Figure 4B). Each stripe is continuous along the dorsal–ventral axis (Figure 4C) in both the ectoderm and the underlying mesoderm (Figure 4B). The stripes persist throughout stage 11 and decay during germband retraction (stage 12). The stripes appear to form just anterior of parasegmental grooves in anterior compartment cells, but precise determination of boundaries is difficult due to weak signal (Figures 4B and 4C, arrowheads).

The accumulation of COS2 in imaginal discs is reminiscent of its expression in the germband-extended embryo. In situ hybridizations with single-stranded sense (Figure 4D) and antisense (Figure 4E) *cos2* probes show that *cos2* mRNA is uniform within wing discs. In contrast, COS2 levels are elevated in the anterior compartment (Figure 4F). A *ptc-lacZ* enhancer trap stock (AT90), producing nuclear-localized β-galactosidase (β-gal) in a *ptc*-specific pattern (Phillips et al., 1990), was used to show that the position of the A/P border (Figure 4G, arrow) corresponds to the line of transition from high to low COS2 levels (Figure 4H, arrow).

The apparent elevation of COS2 in the anterior could be due to higher protein levels, to differential fixation of COS2, or to the accessibility of COS2 to antibodies. We confirmed that the amount of protein is regulated by dissecting anterior and posterior portions of wing discs and measuring protein levels on blots (Figure 4I, [Ant.] and [Post.]). The amount of COS2 (C2), CI, and Engrailed (E) protein was normalized to the amount of α-tubulin (T) in the two fractions. Although COS2 is present in the posterior disc extract, it is less abundant than in the anterior disc extract, in keeping with the histochemical staining result. The COS2 detected in the posterior disc extract has a slower mobility than the anterior protein, suggesting it is a distinct posttranslational form of COS2. As expected, CI and EN were detected only in anterior and posterior disc extracts, respectively (Kornberg et al., 1985; Eaton and Kornberg, 1990; Motzny and Holmgren, 1995; Slusarski et al., 1995).

COS2 and CI Associate with Microtubules in Embryo Extracts

A hallmark of kinesins is the ability to bind taxol-stabilized microtubules (Saxton, 1994). We tested whether COS2 from fly embryos also binds microtubules. Embryo extracts were supplemented with taxol and centrifuged to bring down microtubules and associated proteins. In the absence of taxol (Figure 5A, lane 1), COS2, kinesin heavy chain (KHC), and α-tubulin are in the supernatant. In the presence of taxol, α-tubulin is in the pellet, showing that microtubules have formed efficiently (Figure 5A, compare lanes 4 and 5). While COS2 pellets, KHC remains in the supernatant because kinesin does not bind microtubules in the presence of the ATP contributed by the embryo extract (Lasek and Brady, 1985; Vale et al., 1985). In the presence of the nonhydrolyzable ATP analog AMP-PNP and apyrase, which breaks down ATP, both KHC and COS2 are in the microtubule pellet (Figure 5A, compare lanes 6 and 7). Therefore, COS2 binds microtubules in a taxol-dependent, ATP-insensitive manner, while KHC binds microtubules in a taxol-dependent, ATP-sensitive manner. A bacterially expressed COS2-GST fusion protein, containing the putative motor domain, also binds to purified microtubules (data not shown).

We also tested whether CI associates with microtubules, since so much CI is cytoplasmic. CI associates

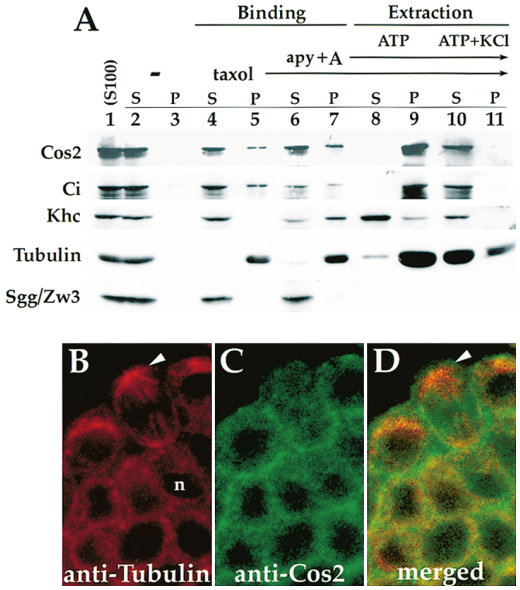

Figure 5. COS2 Binds to Microtubules In Vitro and Overlaps with α-Tubulin in Embryos

(A) Microtubule-binding assays. S100 extracts were either not supplemented ([−], lanes 2 and 3) or supplemented with 40 μM taxol, or 40 μM taxol, 0.5 mM AMP-PNP (A), and 80 U/ml apyrase (apy) (Binding, lanes 4–7). Supernatant (S) and pellet (P) fractions were assayed for COS2, CI, KHC, α-tubulin and SGG/ZW3. The 0.5 M KCl causes most microtubles to dissolve and enter the supernatant (compare lanes 10 and 11).

(B–D) A single scanning confocal micrograph showing indirect immunofluorescence for (B) α-tubulin, (C) COS2, and (D) images (B) and (C) merged. In (B), the three cells shown at the top are undergoing postblastoderm mitoses. An arrowhead indicates a microtubule aster; (n) indicates nucleus. In (C), COS2 is distributed throughout the cytoplasm, showing heightened accumulation along the periphery of some cells. COS2 is not observed on mitotic asters. In (D), yellow indicates overlap between α-tubulin and COS2 within the cytoplasm, COS2 visible at the periphery of cells does not colocalize with α-tubulin. Stage 6 embryo magnified 1100×.

with microtubules just as COS2 does, in a taxol-dependent, ATP-insensitive manner (Figure 5A). The slight amount of CI sedimenting in the absence of taxol is not consistently observed.

The effect of exogenous ATP on COS2 binding to microtubules was tested. Microtubule pellets containing COS2, CI, and KHC were washed and resuspended in the presence of taxol and 5 mM ATP or taxol, 5 mM ATP, and 0.5 M KCl and were then recentrifuged. KHC is partially extracted into the supernatant with just ATP, as expected (Figure 5, compare lanes 8 and 9). However, both COS2 and CI remain microtubule associated in the presence of ATP. COS2, CI, and KHC are completely extracted from microtubules in the presence of 5 mM ATP and 0.5 M KCl (Figure 5, compare lanes 10 and 11). Most microtubules dissolve in the high salt, but some remain intact. Shaggy/Zeste-white3 (SGG/ZW3) protein (Siegfried et al., 1990), a kinase not expected to bind microtubules, serves as a control. A slight amount of SGG/ZW3 cosediments with microtubules (Figure 5, lane 7).

Embryos stained with antibodies to α-tubulin (Figure 5B) and COS2 (Figure 5C) reveal an overlap between COS2 and microtubules, but not a strict colocalization (Figure 5D). Presumably, not all of the COS2 is microtubule associated in vivo, consistent with the in vitro microtubule-binding results (Figure 5A, compare lanes 4 and 5, and 6 and 7).

COS2 and CI Physically Associate

The similar microtubule association of COS2 and CI suggested the two proteins might be in a protein complex. We tested whether COS2 and CI coelute from a gel filtration column. A S100 embryo extract was separated on a Sepharose 4B column, and fractions were assayed for COS2, CI, and α-tubulin by immunoblotting. The elution profiles for COS2 and CI are virtually identical (Figure 6A). Their common peak fraction is approximately 500–600 kDa. A homodimer of COS2 is expected to elute with an approximate peak of 350 kDa. α-tubulin elutes with an apparent molecular weight of 110 kDa, consistent with the expected size of α/β-tubulin heterodimers (Figure 6A). Because microtubules are efficiently depolymerized under the conditions used, the coelution of COS2 and CI is not dependent on microtubule-mediated cross-linking of the two proteins.

We tested whether COS2 and CI are associated in a protein complex using immunoprecipitation. Anti-COS2 and anti-CI antibodies nearly completely precipitate COS2 and CI, respectively (Figure 6B, compare pellets and supernatants). A significant fraction of CI is coprecipitated by anti-COS2 antibodies and vice versa (Figure 6B). COS2 preimmune antisera alone do not precipitate COS2 or CI (Figure 6B), nor do protein G–Sepharose beads alone (not shown).

cos2 Somatic Clones Have Increased Cytoplasmic CI Staining and Cause Pattern Duplications

We employed the FLP recombinase-FRT technique (Xu and Harrison, 1994) to generate homozygous clones of *cos2* in wing discs and examined the subcellular location and expression of CI. Approximately 50% of flies genetically competent to form *cos2* somatic clones display extra wing veins and/or dramatic mirror-image duplications characteristic of *cos2* mutants (Figure 7A) (Grau and Simpson, 1987; Simpson and Grau, 1987). *cos2* clones, marked by the loss of the MYC epitope carried on the homologous chromosome (green in Figure 7), are frequently observed in both the A and P compartments of wing discs. Elevated cytoplasmic CI staining is seen in *cos2* clones in the A compartment (Figures 7B–7D). The level of CI staining is independent of the clone's distance from the A/P border (data not shown) or size (Figure 7C). Nuclear CI is not evident in the clones (Figure 7C). *cos2* clones in the P compartment do not express *ci* (data not shown).

Discussion

COS2 Is a Divergent Member of the Kinesin Gene Family

The COS2 sequence resembles kinesin, but COS2 does not appear to belong to an existing kinesin subfamily

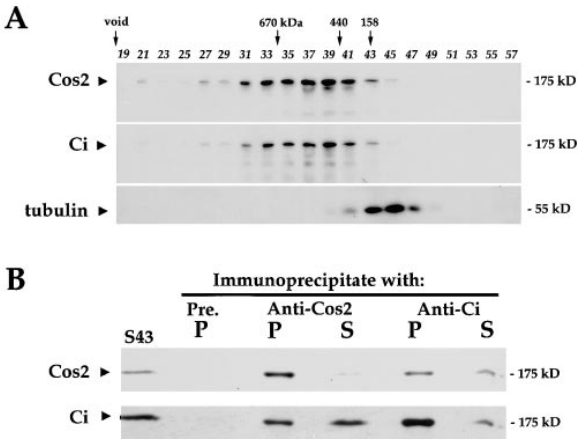

Figure 6. COS2 and CI Are Physically Associated in Exbryonic Extracts

(A) Coelution profile of COS2 and CI from a Sepharose 4B column. The proteins elute in a common peak between 500 and 600 kDa. α-tubulin elutes as a peak at 110 kDa, the expected size for α/β-tubulin heterodimers. Protein standard sizes and elution peak positions are indicated above fraction numbers. The position of the void volumn is indicated at the left; only odd numbered fractions were analyzed.

(B) Immunoblots show pellets (P) and supernatants (S) from coimmunoprecipitations with COS2 antisera (anti-COS2) and CI antisera (anti-CI). COS2 preimmune serum (Pre.) does not precipitate either COS2 or CI. Both COS2 and CI are found in the pellets of immunoprecipitations done using either anti-COS2 or anti-CI antisera. S43 refers to embryo lysate. Blots were probed with either COS2 or CI antibodies as indicated.

and may have novel properties. Phylogenetic subfamilies have been established based on structural and functional similarities between motor domains (reviewed by Goldstein, 1993; Moore and Endow, 1996). Some subfamilies are implicated in microtubule-based vesicle or organelle movement, while others participate in assembly or force generation for mitotic or meiotic microtubule spindles. The motor domain motifs implicated in nucleotide binding in other kinesins are different in COS2, so COS2 may lack motor activity. Most kinesin motor proteins release microtubules when provided with ATP, an intrinsic property of the motor domain (Lasek and Brady, 1985; Vale et al., 1985; Cole et al., 1994). In contrast, COS2 remains attached to microtubules when exogenous ATP is provided. This suggests that unlike kinesin and many kinesin-related proteins, COS2 may not regulate its binding to microtubules by ATP hydrolysis. The nucleotide-binding motifs of COS2 may be unable to coordinate ATP.

The unconventional nature of COS2 is also manifested in its localization in early embryos. Prior to somatic cell formation, COS2 accumulates in a honeycomb pattern at the cortex of the embryo. A similar lattice pattern is characteristic of actin and actin-associated proteins (Miller et al., 1989). Slightly later, during cellularization, COS2 is associated with the actin-rich furrow canals, and with the periphery of cells after cellarization. SMY1, a divergent kinesin-related protein, also localizes to actin-rich regions of the cell (Lillie and Brown, 1994) and has been implicated in two actin-based processes: polarized growth and secretion in yeast (Lillie and Brown, 1992).

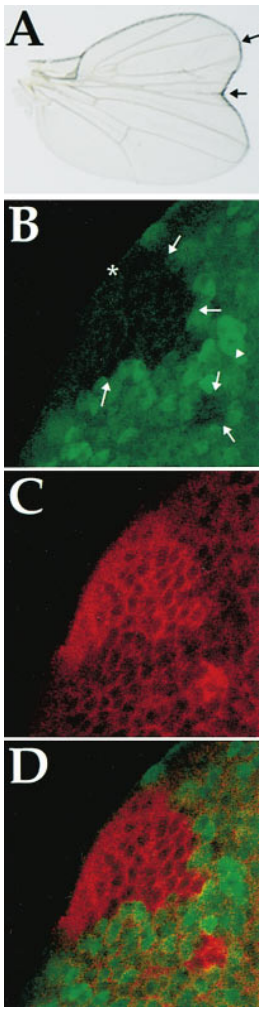

Figure 7. CI Protein Levels Are Elevated in Cells Lacking *cos2* Function

(A) A mirror-image duplication of anterior wing pattern from a P[hsp70-FLP]; P[FRT] $cos2^{W1}$ heat-treated fly. Arrows indicate planes of mirror-image symmetry.

(B–D) These scanning confocal micrographs show a portion of the anterior compartment of a wing disc by indirect immunofluorescence of (B) nuclear localized MYC, (C) cytoplasmic CI, and (D) both (B) and (C) merged. In (B), the absence of MYC expression marks a large $cos2^{W1}/cos2^{W1}$ clone (arrows) along the anterior edge (asterisk) of the disc. A small $cos2^{W1}/cos2^{W1}$ clone is also indicated by arrows. In (C), elevated levels of cytoplasmic CI are seen within both $cos2^{W1}/cos2^{W1}$ clones. MYC does not localize to the nucleolus (arrowhead). Magnified 630×.

COS2 Levels Are Posttranscriptionally Elevated in the Anterior Compartment

Because *cos2* mRNA levels are uniform, the elevated level of COS2 in the A cells must be due to differences between A and P cells in either the production or the stability of COS2. The uniform level of COS2 throughout the anterior compartment of imaginal discs is inconsistent with HH signal regulating its accumulation. HH regulates CI posttranscriptionally in the anterior compartment, but the limited range of HH (Basler and Struhl, 1994; Tabata and Kornberg, 1994) results in a graded distribution of CI across the anterior compartment quite

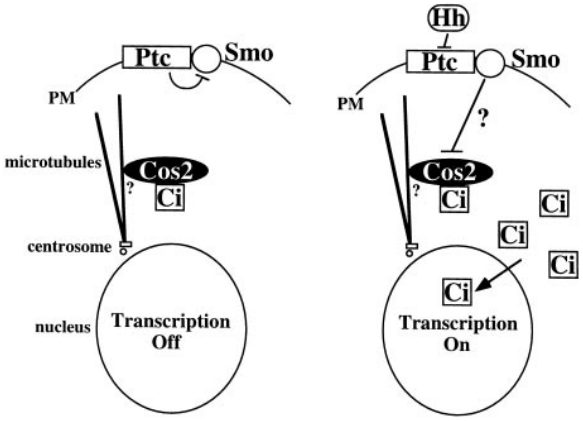

Figure 8. A Model for the COS2/CI Complex in HH Signaling

Diagrams of two adjacent anterior compartment cells are shown; the A/P border is at the right. Both cells express PTC, SMO, FU, COS2, and CI. The known or suspected subcellular localization of each protein is indicated. PTC and SMO are associated in the plasma membrane (PM). COS2 and CI are associated in a cytoplasmic complex. In the absence of HH signal (left cell), PTC inhibits SMO function. COS2 is active, repressing CI levels posttranscriptionally and retaining CI in the cytoplasm (transcription off). In the presence of HH signal (right cell), PTC is directly inhibited by HH, allowing SMO signaling to inhibit COS2 activity either through FU or other cytoplasmic factors (question mark). This triggers CI activation of HH targets (transcription on). The complex may be microtubule-associated through COS2 (small question mark). PKA and SU(FU) function in the pathway, but their relationships to the complex are unknown.

unlike the COS2 distribution (Motzny and Holmgren, 1995; Slusarski et al., 1995). A uniform anterior- or posterior-specific activity could establish the high uniform level of COS2 in the anterior compartment. One possibility is that the moderate level of CI in all A cells is sufficient to stabilize COS2 in a complex. In P cells, COS2 would turn over more rapidly because it is not protected by complex formation. Another possibility is that CI heightens translation of *cos2* mRNA, a possible role for the CI zinc-finger protein in the cytoplasm. Alternatively, a factor controlled by *en* could destroy COS2 in P cells or stabilize it in A cells. *cos2* is not required for patterning the posterior compartment (Whittle, 1976; Grau and Simpson, 1987; Simpson and Grau, 1987), so the low level of COS2 detected in the posterior disc extract may be nonfunctional.

COS2 May Directly Inhibit CI from Activating HH Target Genes

Previous genetic evidence indicates that *cos2* functions in A cells to regulate HH target gene expression (Forbes et al., 1993; Préat et al., 1993; Capdevila et al., 1994; Sanchez-Herrero et al., 1996). Our findings are consistent with these genetic data. First, COS2 accumulates to high levels in A cells. Second, COS2 physically associates with CI, which is expressed in A cells. Third, *cos2* activity reduces CI staining in A cells. *cos2* somatic clones in the anterior compartment of wing discs express high levels of CI and cause mirror-image duplications of the wing. These pattern duplications are predicted to result from CI-mediated activation of *dpp* within *cos2* clones (Capdevila et al., 1994; Sanchez-Herrero et al., 1996). We propose that COS2 and CI act in a large protein complex in the cytoplasm of A cells to mediate the regulation of HH target genes.

The control of HH target gene expression may depend on the level and/or posttranslational form of CI. When increased CI is produced in wing discs far from the A/P border, beyond the influence of HH, *dpp* and *ptc* transcription are activated in A cells (Alexandre et al., 1996; Dominguez et al., 1996; Hepker et al., 1997). Because *dpp* and *ptc* are also activated in P cells, the CI-mediated activation of these targets does not depend on an A compartment–specific factor. CI may normally require a HH-dependent modification to activate HH targets, but elevated CI seems sufficient to activate HH targets. Along the A/P border CI levels are posttranscriptionally elevated in response to HH signaling (Johnson et al., 1995; Slusarski et al., 1995; Hepker et al., 1997). This elevated level of CI is thought to allow it to enter the nucleus and directly activate HH targets (Alexandre et al., 1996; Dominguez et al., 1996; Hepker et al., 1997). Although endogenous CI is hard to see in the nucleus, when the C-terminal portion of an epitope-tagged CI is removed, leaving the zinc fingers intact, CI protein appears in the nucleus and the cytoplasm (Hepker et al., 1997). CI therefore appears competent to enter the nucleus but is normally restricted to the cytoplasm by the C-terminal tail. The absence of detectable CI in the nucleus may be the result of inadequate CI antibodies.

The protein complex we have identified could control the level of CI and its subcellular distribution. The COS2/CI complex may control the level of CI either by increasing CI production or decreasing its degradation. The complex could protect CI from proteases only when HH signal is received, or the complex could associate with polysomes to facilitate translation of *ci* mRNA. Because a substantial fraction of COS2 and CI are associated, COS2 may sequester CI in the cytoplasm, possibly by tethering it to the cytoskeleton (Figure 8). Because CI lacks an obvious nuclear localization signal (Orenic et al., 1990; Motzny and Holmgren, 1995) its movement to the nucleus may be regulated by its ability to couple to a protein that carries it there. The transcription factor dCBP may serve this function (Akimaru et al., 1997). COS2 may render CI unavailable to such a protein except along the A/P border, where COS2 is inhibited. The absence of detectable nuclear CI in cells lacking *cos2* function may indicate the need for a second activating event in addition to a release from COS2. CI may have to be modified to be activated, or it may be tethered to a COS2-independent complex, or transport into the nucleus may require an activated cofactor. Alternatively, nuclear CI may be masked from the antibodies used.

The identification of the COS2/CI complex helps to fill in missing steps in HH signaling by showing direct interactions among two of the five known signal transduction components and by providing a cytoskeletal link. The importance of the complex is further underscored by the presence of a third component, *fused* (Robbins et al., 1997 [this issue of *Cell*]). The subcellular distribution of the complex may be important for controlling HH targets and, consequently, cell differentiation.

Materials and Methods

Molecular Cloning and Hybridizations

Molecular biology techniques were carried out according to Sambrook et al. (1989). The *cos2* chromosome walk was initiated with a genomic clone (λB47, kindly provided by Dr. Ed Stephenson) and using a cosmid library (Tamkun et al., 1992) made from an isogenic fly stock (iso-1). The progress of the walk and positions of deficiencies were determined by in situ hybridization of biotin-labeled DNA fragments to polytene chromosomes (Pardue, 1994). Overlapping iso-1 genomic λ phage clones lying between *Df(2R)sple*^{D1} and *Df(2R)NCX11* were isolated, and positions of *cos2* mutations were determined using blots of *cos2* mutant genomic DNA. From 38 *cos2* cDNA clones recovered from a λgt10, 0–3 hr embryonic cDNA library (Poole et al., 1985) and a plasmid-based imaginal disc cDNA library (Brown and Kafatos, 1988), two approximately full-length clones, D12 and D13, were found and sequenced. In situ hybridization of riboprobes to embryos and imaginal discs was carried out as described (Mathies et al., 1994).

Germline Transformations

The 6.1 kb KpnI (K6.1) and 9.5 kb HindIII (H9.5) genomic fragments were subcloned into pCaSpeR4. Transgenic flies were made according to Spradling and Rubin (1982), using *w*^{1118} embryos as recipients. Seven independent K6.1 inserts and eight independent H9.5 inserts were recovered. Rescue crosses were done at 25°C.

Antibody Preparation and Immunoblotting

Affinity-purified rat polyclonal antisera were prepared to two parts of COS2. A 1.5 kb SacI–EcoRI (SR1.5) fragment, including the putative motor domain, and a 0.8 kb EcoRI (R0.8) fragment, including the N-terminal 19 heptad repeats, were each subcloned into two different plasmid expression vectors, pATH10 (Rimm and Pollard, 1989) and pGEX-2T (128/129) (kindly provided by Dr. M. Blanar). The pATH10 clones create E. coli TRPE-COS2 fusion proteins, which were used as immunogens. Each TRPE-COS2 fusion protein was purified from the BL21 p*Lys*S cell lysates as inclusion bodies, cut from SDS gels, and injected into rats (Josman Labs). The pGEX-2T (128/129) clones create glutathione S-transferase (GST)-COS2 fusion proteins, which were used to affinity purify the rat antisera. Soluble GST-COS2 fusion proteins were purified from BL21 p*Lys*S cells using glutathione-agarose beads and coupled to AminoLink Plus chromatography columns (Pierce). Antibodies were eluted from columns with 4.5 M $MgCl_2$ and dialyzed against 50 mM HEPES (pH 7.5), 150 mM NaCl, 1 mM EDTA, and 0.01% NaN_3.

Immunoblots were carried out as described by Harlow and Lane (1988). After 7.5% SDS–PAGE, proteins were transferred to Protran membrane (Schleicher and Schuell), and membranes were blocked with 5% nonfat dry milk for 2–6 hr. Antibodies used are as follows: COS2, rat polyclonal antisera (1:50); CI, rat monoclonal (1:15, gift of Dr. B. Holmgren); α-tubulin, mouse monoclonal (1:100, gift of Drs. R. Sakowizc and L. Goldstein); EN, mouse monoclonal (1:500, gift of Dr. T. Kornberg); DmKhc, DK410-7.1 mouse monoclonal (1:50, gift of Drs. R. Sakowicz and L. Goldstein); SGG/ZW3, rabbit polyclonal (1:500, gift of Dr. K. Willert); and all Horseradish Peroxidase (HRP)–conjugated secondary antibodies (1:20,000, Jackson ImmunoResearch Labs). HRP was detected with Chemiluminescence reagent (NEN).

Anterior or posterior fragments of wing discs were dissected from third instar larvae and transferred to 40 mM Tris (pH 7.2), 250 mM NaCl, 5 mM EDTA, and 0.05% NP-40 on ice, 0.5 fragments/μl. Fragments were stored at −80°C, thawed, and homogenized. Approximately 70 anterior and posterior disc fragment equivalents were analyzed by immunoblotting.

Protein Detection in Embryos and Discs

Washed and dechorionated embryos were fixed, as described, with either heat and methanol (Miller et al., 1989), methanol (Kellogg et al., 1989), or formaldehyde (Theurkauf, 1992). After fixation, embryos were stored either at −20°C in methanol or taken through a rehydration series to prepare embryos for indirect immunofluorescence. Third instar larval imaginal discs were prepared for indirect immunofluorescence as described by Johnson et al. (1995). Samples were mounted in Vectashield H-1000 (Vector Laboratories Inc.) and examined by confocal microscopy. Antibodies used are as follows: COS2, rat polyclonal antisera (1:5); α-tubulin, mouse monoclonal (1:25, gift of Drs. R. Sakowizc and L. Goldstein); lamin, mouse monoclonal (1:40, gift of Drs. B. Harmon and J. Sedat); β-gal, rabbit polyclonal (1:100, Cappel); and all fluorescent secondary antibodies (1:200, Jackson ImmunoResearch Labs).

Microtubule-Binding Assays

This assay was carried out according to Kellogg et al. (1989), with some modifications. Briefly, 16 g of 2–10 hr Canton S embryos were homogenized in 32 ml of C buffer (50 mM HEPES [pH 7.6], 1 mM $MgCl_2$, 1 mM EGTA), 0.5 mM DTT, and protease inhibitors (1.74 μg/ml PMSF, 1 mM benzamidine, 2 μg/ml aprotinin, 1 μg/ml leupeptin, 1 μg/ml pepstatin, all from Sigma) on ice. A supernatant (S100) was prepared, and five 5 ml aliquots were made. One aliquot received 40 μM taxol (Sigma) and 1 mM GTP (binding, lanes 4 and 5); three aliquots received 40 mM taxol, 1 mM GTP, 80 U/ml apyrase (Sigma), and 0.5 mM AMP-PNP (Boehringer-Mannheim) (binding, lanes 6 and 7, and extractions); and one was not supplemented (−taxol). Aliquots were incubated at 25°C for 20 min and then on ice for 10 min. Each sample (4 ml) was layered over a 10% sucrose cushion and centrifuged at 48,000 × g for 30 min at 4°C. For the −taxol and both binding samples, supernatants were saved, and pellets were washed and resuspended in 4.5 ml of CX buffer (C buffer supplemented with 10% glycerol, 25 mM KCl, and protease inhibitors). For the extraction samples, pellets were resuspended in 1 ml of CX buffer (supplemented with 40 μM taxol, 1 mM GTP, and either 5 mM Mg-ATP or 5 mM Mg-ATP and 0.5 M KCl) and incubated on ice for 10 hr before centrifugation, as before. The resulting supernatants were saved, and pellets were resuspended in 1 ml of CX buffer. Each sample (15 μl in 1X sample buffer) was separated by SDS–PAGE and immunoblotted.

Chromatography

A Sepharose 4B (Pharmacia) column (48.5 cm × 1.77 cm^2 equaling a bed volumn [V_t] of 86 ml and a void volumn [V_o] of 28.5 ml) was calibrated with protein standards (Pharmacia) and operated at a pressure head of 64 cm with a flow rate of 17.5 ml/hr. Embryos were homogenized in TNE buffer (40 mM Tris [pH 7.2], 250 mM NaCl, 0.5 mM EDTA, 10% glycerol, 0.05% NP-40, and 1 μg/ml nocodazole) + proteinase inhibitors (previously listed), and an S100 protein extract was prepared as above and dialyzed against column running buffer overnight at 4°C. The S100 was recentrifuged at 100,000 × g for 30 min at 4°C. The total protein concentration of the resulting S100 (34 mg/ml) was determined, and 250 μl (8.5 mg) was loaded onto the column. Column runs were monitored by a UV spectophotometer at OD_{A280}, and 1.5 ml fractions were collected. Proteins were precipitated with acetone and analyzed by immunoblot.

Coimmunoprecipitation

An embryonic extract (S43) prepared in TNE buffer + proteinase inhibitors was preincubated with protein G–Sepharose beads (Pharmacia) for 30 min at 4°C with rocking. Beads were pelleted in a microfuge (30 sec), and the pellet was saved for immunoblotting. Aliquots (100 μl) of the supernatant were transferred to fresh tubes and supplemented with 1 μl of rat polyclonal COS2 antisera, 1 μl of rabbit polyclonal CI antisera (gift of Dr. T. Kornberg), or 1 μl of preimmune sera, and then rocked at 4°C for 30 min. Protein G–Sepharose beads were added and samples rocked for 2 hr at 4°C. Beads pelleted as before were washed three times with TNE buffer. Washed beads were centrifuged, and pellets and supernatants were examined by immunoblotting.

Somatic clones

cos2 mutant clones were made with *cos2*^{W1} (Whittle, 1976). Both P[*w*$^+$; FRT]^{G13} *cos2*^{W1}/*CyO* flies and P[*w*$^+$; FRT]^{G13} P[hsp70-MYC] (G13-πM) flies were crossed separately with *yw* P[*ry*$^+$; FLP]^{12}; *CyO*/*Sco* flies. *yw* P[*ry*$^+$; FLP]^{12}; P[*w*$^+$; FRT]^{G13} *cos2*^{W1}/*CyO* and *yw* P[*ry*$^+$; FLP]^{12}; G13-πM/*CyO* siblings were crossed, and after two days, adults were transferred to fresh vials. Larvae were heat-shocked on days 2, 3, and 4 for one hour at 37°C. Imaginal discs were dissected from third instar larvae 30 min after a fourth one-hour heat shock.

Discs were incubated with monoclonal antibodies 9E10 anti-MYC (Sigma, 1:500) and 2A1 anti-CI (gift of Dr. B. Holmgren, 1:5) and prepared for indirect immunofluorescence.

Acknowledgments

Correspondence regarding this paper should be addressed to M. P. S. (e-mail: scott@cmgm.stanford.edu). We sincerely thank P. Simpson, M. Bourouis, and P. Heitzler for providing the *cos2* fly stocks, which were essential in cloning *cos2*. We thank R. Johnson, R. Nusse, and O. Papoulas for suggestions on the manuscript and M. Fuller, L. Goldstein, R. Sakowicz, and B. Holmgren for helpful discussions. We are also grateful to D. Gubb, J. Tamkun, C. Goodman, Ed Stephenson, M. Blanar, H. Goodson, B. Holmgren, T. Kornberg, K. Willert, B. Dalby, R. Sakowicz, L. Goldstein, B. Harmon, Y. Bellaiche, T. Chou, N. Perrimon, J. Sedat, R. Mayo, W. Smith, and F. Harris for materials and help and to D. Lee, J. J. Plecs and T. Alber for advice. The Stanford PAN facility helped with DNA sequencing. This work was initiated with the support of a grant from the American Cancer Society. K. H. is supported by a National Science Foundation predoctoral grant. M. P. S. is an investigator, and J. C. S. an associate, of the Howard Hughes Medical Institute.

Received February 7, 1997; revised June 6, 1997.

References

Akimaru, H., Chen, Y., Dai, P., Hou, D.-X., Nonaka, M., Smolik, S.M., Armstrong, S., Goodman, R.H., and Ishii, S. (1997). Drosophila CBP is a co-activator of *cubitus interruptus* in *hedgehog* signalling. Nature *386*, 735–738.

Alcedo, J., Ayzenzon, M., Von Ohlen, T., Noll, M., and Hooper, J.E. (1996). The Drosophila *smoothened* gene encodes a seven-pass membrane protein, a putative receptor for the *hedgehog* signal. Cell *86*, 221–232.

Alexandre, C., Jacinto, A., and Ingham, P.W. (1996). Transcriptional activation of *hedgehog* target genes in Drosophila is mediated directly by the *cubitus interruptus* protein, a member of the GLI family of zinc finger DNA-binding proteins. Genes Dev. *10*, 2003–2013.

Ashburner, M. (1989) Drosophila: A Laboratory Handbook (Cold Spring Harbor, NY: Cold Spring Harbor Laboratory Press).

Basler, K., and Struhl, G. (1994) Compartment boundaries and the control of *Drosophila* limb pattern by *hedgehog* protein. Nature *368*, 208–214.

Brown, N.H., and Kafatos, F.C. (1988). Functional cDNA libraries from Drosophila embryos. J. Mol. Biol. *203*, 425–437.

Campos-Ortega, J.A., and Hartenstein, V. (1985). The Embryonic Development of Drosophila melanogaster (Springer-Verlag).

Capdevila, J., Estrada, M.P., Sánchez-Herrero, E., and Guerrero, I. (1994). The Drosophila segment polarity gene *patched* interacts with *decapentaplegic* in wing development. EMBO J. *13*, 71–82.

Cavener, D.R. (1987). Comparison of the consensus sequence flanking translational start sites in Drosophila and vertebrates. Nucleic Acids Res. *15*, 1353–1361.

Cole, D.G., Saxton, W.M., Sheehan, K.B., and Scholey, J.M. (1994). A "slow" homotetrameric kinesin-related motor protein purified from Drosophila embryos. J. Biol. Chem. *269*, 22913–22916.

Dominguez, M., Brunner, M., Hafen, E., and Basler, K. (1996). Sending and receiving the *hedgehog* signal: control by the Drosophila Gli protein Cubitus interruptus. Science *272*, 1621–1625.

Eaton, S., and Kornberg, T.B. (1990). Repression of *ci-D* in posterior compartments of Drosophila by *engrailed*. Genes Dev. *4*, 1068–1077.

Foe, V.E., Odell, G.M., and Edgar, B.A. (1993). Mitosis and Morphogenesis in the Drosophila Embryo: Point and Counterpoint. In The Development of Drosophila melanogaster, M. Bate and A. Martinez Arias, eds. (Cold Spring Harbor, NY: Cold Spring Harbor Laboratory Press), pp. 149–300.

Forbes, A.J., Nakano, Y., Taylor, A.M., and Ingham, P.W. (1993). Genetic analysis of *hedgehog* signalling in the Drosophila embryo. Development *119* (Suppl.), 115–124.

Goldstein, L.S. (1993). With apologies to Scheherazade: tails of 1001 kinesin motors. Annu. Rev. Genet. *27*, 319–351.

Grau, Y., and Simpson, P. (1987). The segment polarity gene *costal-2* in Drosophila. I. The organization of both primary and secondary embryonic fields may be affected. Dev. Biol. *122*, 186–200.

Hammerschmidt, M., Brook, A., and McMahon, A.P. (1997). The world according to *hedgehog*. Trends Genet. *13*, 14–21.

Harlow, E., and Lane, D. (1988). Antibodies: A Laboratory Manual (Cold Spring Harbor, NY: Cold Spring Harbor Laboratory).

Heitzler, P., Coulson, D., Saenz-Robles, M.T., Ashburner, M., Roote, J., Simpson, P., and Gubb, D. (1993). Genetic and cytogenetic analysis of the 43A-E region containing the segment polarity gene *costa* and the cellular polarity genes *prickle* and *spiny-legs* in Drosophila melanogaster. Genetics *135*, 105–115.

Hepker, J., Wang, Q.T., Motzny, C.K., Holmgren, R., and Orenic, T.V. (1997). Drosophila *cubitus interruptus* forms a negative feedback loop with *patched* and regulates expression of *Hedgehog* target genes. Development *124*, 549–558.

Higgins, D.G., Bleasby, A.J., and Fuchs, R. (1992). CLUSTAL V: improved software for multiple sequence alignment. CABIOS *8*, 189–191.

Hooper, J.E., and Scott, M.P. (1989). The Drosophila *patched* gene encodes a putative membrane protein required for segmental patterning. Cell *59*, 751–765.

Ingham, P.W., and Fietz, M.J. (1995). Quantitative effects of *hedgehog* and *decapentaplegic* activity on the patterning of the Drosophila wing. Curr. Biol. *5*, 432–440.

Jiang, J., and Struhl, G. (1995). Protein kinase A and Hedgehog signaling in Drosophila limb development. Cell *80*, 563–572.

Johnson, R.L., Grenier, J.K., and Scott, M.P. (1995). *patched* overexpression alters wing disc size and pattern: transcriptional and post-transcriptional effects on *hedgehog* targets. Development *121*, 4161–4170.

Kellogg, D.R., Field, C.M., and Alberts, B.M. (1989). Identification of microtubule-associated proteins in the centrosome, spindle, and kinetochore of the early Drosophila embryo. J. Cell Biol. *109*, 2977–2991.

Kornberg, T., Siden, I., O'Farrell, P., and Simon, M. (1985). The *engrailed* locus of Drosophila: in situ localization of transcripts reveals compartment-specific expression. Cell *40*, 45–53.

Lasek, R.J., and Brady, S.T. (1985). Attachment of transported vesicles to microtubules in axoplasm is facilitated by AMP-PNP. Nature *316*, 645–647.

Lepage, T., Cohen, S.M., Diaz-Benjumea, F.J., and Parkhurst, S.M. (1995). Signal transduction by cAMP-dependent protein kinase A in *Drosophila* limb patterning. Nature *373*, 711–715.

Li, W., Ohlmeyer, J.T., Lane, M.E., and Kalderon, D. (1995). Function of protein kinase A in Hedgehog signal transduction and Drosophila imaginal disc development. Cell *80*, 553–562.

Lillie, S.H., and Brown, S.S. (1992). Suppression of a myosin defect by a kinesin-related gene. Nature *356*, 358–361.

Lillie, S.H., and Brown, S.S. (1994). Immunofluorescence localization of the unconventional myosin, Myo2p, and the putative kinesin-related protein, Smy1p, to the same regions of polarized growth in Saccharomyces cerevisiae. J. Cell Biol. *125*, 825–842.

Mathies, L.D., Kerridge, S., and Scott, M.P. (1994). Role of the *teashirt* gene in Drosophila midgut morphogenesis: secreted proteins mediate the combinatorial action of homeotic genes. Development *120*, 2799–2809.

Miller, K.G., Field, C.M., and Alberts, B.M. (1989). Actin-binding proteins from Drosophila embryos: a complex network of interacting proteins detected by F-actin affinity chromatography. J. Cell Biol. *109*, 2963–2975.

Moore, J.D., and Endow, S.A. (1996). Kinesin proteins: a phylum of motors for microtubule-based motility. BioEssays *18*, 207–219.

Motzny, C.K., and R. Holmgren (1995). The Drosophila *cubitus interruptus* protein and its role in the *wingless* and *hedgehog* signal transduction pathways. Mech. Dev. *52*, 137–150.

Nakano, Y., Guerrero, I., Hidalgo, A., Taylor, A., Whittle, J.R.S., and

Ingham, P.W. (1989). A protein with several possible membrane-spanning domains encoded by the *Drosophila* segment polarity gene *patched*. Nature *341*, 508–513.

O'Connell, P., and Rosbash, M. (1984). Sequence, structure and codon preference of the Drosophila *ribosomal protein 49* gene. Nucleic Acids Res. *12*, 5495–5513.

Orenic, T.V., Slusarski, D.C., Kroll, K.L., and Holmgren, R.A. (1990). Cloning and characterization of the segment polarity gene *cubitus interruptus Dominant* of Drosophila. Genes Dev. *4*, 1053–1067.

Pan, D., and Rubin, G.M. (1995). cAMP-dependent protein kinase and *hedgehog* act antagonistically in regulating *decapentaplegic* transcription in Drosophila imaginal discs. Cell *80*, 543–552.

Pardue, M.-L. (1994). Looking at polytene chromosomes. In Drosophila melanogaster: Practical Uses in Cell and Molecular Biology, Volume 44, L.S.B Goldstein and E.A. Fyrberg, eds. (San Diego, CA: Academic Press), pp. 333–351.

Phillips, R.G., Roberts, I.J.H., Ingham, P.W., and Whittle, J.R.S. (1990). The Drosophila segment polarity gene *patched* is involved in a position-signalling mechanism in imaginal discs. Development *110*, 105–114.

Poole, S.J., Kauvar, L.M., Drees, B., and Kornberg, T. (1985). The *engrailed* locus of Drosophila: structural analysis of an embryonic transcript. Cell *40*, 37–43.

Préat, T., Thérond, P., Lamour-Isnard, C., Limbourg-Bouchon, B., Tricoire, H., Erk, I., Mariol, M.C., and Busson, D. (1990). A putative serine/threonine protein kinase encoded by the segment-polarity *fused* gene of Drosophila. Nature *347*, 87–89.

Préat, T., Thérond, P., Limbourg-Bouchon, B., Pham, A., Tricoire, H., Busson, D., and Lamour-Isnard, C. (1993). Segmental polarity in Drosophila melanogaster: genetic dissection of *fused* in a *Suppressor of fused* background reveals interaction with *costal-2*. Genetics *135*, 1047–1062.

Rimm, D.L., and Pollard, T.D. (1989). New plasmid vectors for high level synthesis of eukaryotic fusion proteins in E. coli. Gene *75*, 323–327.

Robbins, D.J., Nybakken, K.E., Kobayashi, R., Sisson, J.C., Bishop, J.M., and Thérond, P.P. (1997). Hedgehog elicits signal transduction by means of a large complex containing the kinesin-related protein Costal2. Cell, this issue, *90*, 225–234.

Sablin, E.P., Kull, F.J., Cooke, R., Vale, R.D., and Fletterick, R.J. (1996). Crystal structure of the motor domain of the kinesin-related motor *ncd*. Nature *380*, 555–559.

Sambrook, J., Fritsch, E.F., and Maniatis, T. (1989). Molecular Cloning: A Laboratory Manual (Cold Spring Harbor, NY: Cold Spring Harbor Press).

Sanchez-Herrero, E., Couso, J.P., Capdevila, J., and Guerrero, I. (1996). The *fu* gene discriminates between pathways to control *dpp* expression in Drosophila imaginal discs. Mech. Dev. *55*, 159–170.

Saxton, W.M. (1994). Isolation and analysis of microtubule motor proteins. In Drosophila melanogaster: Practical Uses in Cell and Molecular Biology, Volume 44, L.S.B. Goldstein and E.A. Fyrberg, eds. (San Diego, CA: Academic Press), pp. 279–288.

Siegfried, E., Perkins, L.A., Capaci, T.M., and Perrimon, N. (1990). Putative protein kinase product of the *Drosophila* segment-polarity gene *zeste-white3*. Nature *345*, 825–829.

Simpson, P., and Grau, Y. (1987). The segment polarity gene *costal-2* in Drosophila. II. The origin of imaginal pattern duplications. Dev. Biol. *122*, 201–209.

Slusarski, D.C., Motzny, C.K., and Holmgren, R. (1995). Mutations that alter the timing and pattern of *cubitus interruptus* expression in Drosophila melanogaster. Genetics *139*, 229–240.

Spradling, A.C., and Rubin, G.M. (1982). Transposition of cloned *P* elements into Drosophila germ line chromosomes. Science *218*, 341–347.

Tabata, T., and Kornberg, T. (1994). Hedgehog is a signaling protein with a key role in patterning Drosophila imaginal discs. Cell *76*, 89–102.

Tamkun, J.W., Deuring, R., Scott, M.P., Kissinger, M., Pattatucci, A.M., Kaufman, T.C., and Kennison, J.A. (1992). *brahma*: a regulator of Drosophila homeotic genes structurally related to the yeast transcriptional activator SNF2/SWI2. Cell *68*, 561–572.

Thérond, P., Busson, D., Guillemet, E., Limbourg-Bouchon, B., Préat, T., Terracol, R., Tricoire, H., and Lamour-Isnard, C. (1993). Molecular organisation and expression pattern of the segment polarity gene *fused* of Drosophila melanogaster. Mech. Dev. *44*, 65–80.

Thérond, P.P., Knight, J.D., Kornberg, T.B., and Bishop, J.M. (1996). Phosphorylation of the *fused* protein kinase in response to signaling from *hedgehog*. Proc. Natl. Acad. Sci. USA *93*, 4224–4228.

Theurkauf, W.E. (1992). Behavior of structurally divergent alpha-tubulin isotypes during Drosophila embryogenesis: evidence for post-translational regulation of isotype abundance. Dev. Biol. *154*, 205–217.

Vale, R.D. (1996). Switches, latches, and amplifiers: common themes of G proteins and molecular motors. J. Cell Biol. *135*, 291–302.

Vale, R.D., Reese, T.S., and Sheetz, M.P. (1985). Identification of a novel force-generating protein, kinesin, involved in microtubule-based motility. Cell *42*, 39–50.

van den Heuvel, M., and Ingham, P.W. (1996). *smoothened* encodes a receptor-like serpentine protein required for *hedgehog* signalling. Nature *382*, 547–551.

Whittle, J.R.S. (1976). Clonal analysis of a genetically caused duplication of the anterior wing in Drosophila melanogaster. Dev. Biol. *51*, 257–268.

Woehlke, G., Rudy, A.K., Hart, C.L., Ly, B., Hom-Booher, N., and Vale, R.D. (1997). Microtubule interaction site of the kinesin motor. Cell, this issue, *90*, 207–216.

Woolfson, D.N., and Alber, T. (1995). Predicting oligomerization states of coiled coils. Protein Sci. *4*, 1596–1607.

Xu, T., and Harrison, S.D. (1994). Mosaic analysis using FLP recombinase. In Drosophila melanogaster: Practical Uses in Cell and Molecular Biology, Volume 44, L.S.B. Goldstein and E.A. Fyrberg, eds. (New York: Academic Press), pp. 655–681.

Yang, J.T., Saxton, W.M., Stewart, R.J., Raff, E.C., and Goldstein, L.S. (1990). Evidence that the head of kinesin is sufficient for force generation and motility in vitro. Science *249*, 42–47.